Received January 2002
Revised November 2003
Accepted November 2003

Design optimization of an air-filled cavity

Control of the constrained maximum temperature at the directly heated vertical wall

Antonio Campo
Department of Mechanical Engineering, The University of Vermont, Burlington, Vermont, USA
Mark D. Landon
College of Engineering, Idaho State University, Pocatello, Idaho, USA

Keywords *Electrical components, Convection, Cavitation, Optimization techniques*

Abstract *A review of the literature reveals that the optimal shape of natural convective cavities has not been investigated so far. A prominent application of cavities cooled by natural convection arises in the miniaturization of electronic packaging where some type of temperature constraint must be applied at the directly heated wall. This contemporary issue has been addressed in the present work in an elegant manner by linking a code on computational fluid dynamics with a shape optimization code. Once the velocity and temperature fields were accurately computed for an initial cavity with a certain heat load, a two-step optimization procedure was implemented in a methodical fashion. A first optimization sub-problem transformed a square cavity into a rectangular cavity, while the second optimization sub-problem sculpted the shape of the upper horizontal insulated wall in order to bring down the maximum wall temperature of the directly heated vertical wall, i.e. the so-called "hot spot". A bird's eye inspection of the numerical results revealed that the first optimization sub-problem produced a significant reduction in area (volume), while raising the maximum wall temperature of the heated vertical wall by a small amount. The second optimization sub-problem supplied a remarkable decrease in the maximum wall temperature of the heated vertical wall, carrying with it a moderate increase in area (volume). At the end, the optimal shape of the cavity turns out to be a disfigured vertical rectangular cavity in which the upper insulated wall forming a parabolic-skewed cap.*

Nomenclature

A = aspect ratio of cavity, H/W
c_p = specific isobaric heat capacity, J/kg C
g = acceleration of gravity, m/s^2
h = local convective coefficient of internal fluid, W/m^2 C
$\bar{h}$ = average convective coefficient of internal fluid, W/m^2 C
$\bar{h}_e$ = average convective coefficient of external fluid at the right vertical wall, W/m^2 C
H = cavity height, m
k = thermal conductivity, W/m C
Nu_x = local Nusselt number, hx/k
$\overline{Nu}_H$ = average Nusselt number, $\bar{h}H/k$
p = pressure, Pa
Pr = Prandtl number, $\mu c_p/k$
q_w = applied heat flux at the left vertical wall, W/m^2
Ra_H = modified Rayleigh number, $g(\beta/k\nu^2)q_w H^4$
T = temperature, C
T_∞ = temperature of external fluid, C
u, v = velocities in the x- and y-directions, m/s
x, y = coordinates, m
W = cavity width, m

International Journal of Numerical Methods for Heat & Fluid Flow
Vol. 14 No. 6, 2004
pp. 718-733

0961-5539
DOI 10.1108/09615530410544274

Greek letters

β = isobaric coefficient of volumetric thermal expansion, 1/K

μ = dynamic viscosity, $N s/m^2$

ν = kinematic viscosity, m^2/s

ρ = density, kg/m^3

1. Introduction

The study of natural convection in four-sided cavities has been and continues to be an area of considerable interest from the joined standpoint of fundamental and applied research in fluid dynamics and heat transfer (Gebhart *et al.*, 1988; Raithby and Hollands, 1998). The motion of a fluid is usually induced in a stationary cavity even when small temperature differences are applied at the thermally active walls. Heat transfer through the cavity walls causes density changes to the confined fluid. This action leads to buoyancy-driven fluid circulation resulting in velocity fields that are highly dependent on the temperature fields. A set of varying design parameters in natural convection cavities normally determines the flow structure and the cavity performance for specific industrial tasks. This scenario represents an important type of buoyant flows occurring in various branches of engineering, geophysics, environmental sciences, etc.

Natural convection affords a gratifying means of thermal management of computer systems that eliminates the fan or the pump, and consequently provides a pleasant environment free of noise and vibration. The study of heat transfer from arrays of discrete heat sources mounted on a wall of cavities is motivated by specialized applications in the cooling of electronic components. Heat dissipation of chips is continually increasing in modern electronic equipment as a result of expanding circuit integration and power. In addition, miniaturization of electronic devices has played a decisive role in modern era because the heat flux density has increased beyond the levels encountered earlier in electronic technology. Since the maximum allowable chip temperatures for electronic devices are limited by different requirements, a variety of novel hydrodynamic and thermal control techniques have evolved in the past to meet strict temperature criteria in industry (Peterson and Ortega, 1990). Many different schemes have been discussed in state-of-the-art review articles and do not need to be repeated here.

The present study was motivated by the need for miniaturization of passive cooling systems that use closed cavities with natural convection heat removal. In this regard, attention has been focused on the temperature rise of the directly heated vertical wall of a cavity and the imminent desire to lower it. In square or vertical rectangular cavities, the hot fluid flows upward parallel to the vertical heated wall. The fluid starts to turn away from the heated wall and moves toward the upper horizontal insulated wall well below reaching the corner. This change in direction results in a reduction of convective heat transport in the vicinity of the corner that sees a heat flux discontinuity. The fulfillment of a design objective may necessitate the alteration of the shape of one (or more) of the walls that conform the cavity. Although contemporary codes on computational fluid dynamics can predict the thermal management of natural convective cavities of fixed shapes, these codes do not offer any significant insight into how to improve the performance by varying the design parameters. Generally, the design engineer has to resort to experience, intuition and experimentation to improve the thermal performance of cavities in a laborious trial-and-error manner. Some of the

design parameters of cavity flows are related to the geometrical shape and these elements are difficult to determine beforehand. As a result, shape optimization has become a major area of research in design engineering. Focusing our attention on natural convection cavities, the shape optimization seeks to mathematically determine the best set of design parameters that are capable of providing the highest thermal performance of cavities subjected to certain constraints.

The body of the paper is divided into four sections. In Section 2, the physical system and the mathematical formulation are addressed. The computational procedure and the code validation are explained in Section 3. Section 4 is devoted to the shape optimization algorithm. Finally, Section 5 contains a test problem, a discussion of the numerical velocity and temperature fields, and the revelation of the optimal shape of the cavity.

1.1 Literature review

There is a wealth of technical publications that have dealt with natural convection cavity flows in the past. From a historical perspective, the earliest investigation on this kind of confined flow was done by Batchelor (1954). This author considered cavities with large aspect ratios $A = H/W$ ranging from about 5 to ∞ and fluid flows are characterized by small Rayleigh numbers. The conclusion was that, if A is large, there was a small increase in the heat transfer over that due to conduction alone for $\mathrm{Ra} < 1{,}000$. Additionally, conduction was also shown to be the mechanism of heat transfer for large aspect ratios, i.e. $A \rightarrow \infty$ associated with any Ra. For large Ra, the core or the central region of the rectangular cavity away from the vertical boundary layers adjacent to the walls was assumed to be isothermal. The prominent experimental studies of Eckert and Carlson (1961) and Elder (1965) convincingly confirmed for the first time that the core region of the cavities was relatively stagnant and the temperature was almost linearly stratified.

Actual cavities occurring in engineering practice often have their shapes differing from the conventional square, rectangular or polygonal geometry that are customarily used in theoretical and experimental studies. There have been considerable advances in the study of natural convection in cavities of arbitrary shape due to the development of efficient computational methods for solving the Navier-Stokes and energy equations in non-Cartesian coordinates, e.g. the finite element method and the finite difference method with embedded boundary fitted coordinates (Raithby and Hollands, 1998). In this broad context, numerous studies have looked at a wide variety of cavity configurations and the list of references (Akinsete and Coleman, 1982; Asako and Nakamura, 1982; Chang *et al.*, 1982; Chung and Trefethen, 1982; Facas, 1993; Holtzman *et al.* 2000; Hyun and Choi, 1990; Iyican *et al.*, 1980a, b; Karyakin *et al.*, 1988; Kim and Hyun, 1999; Lam *et al.*, 1989; Lee, 1984, 1991; Maekawa and Tanasawa, 1982; Naylor and Oosthuizen, 1994; Nithiarasu *et al.*, 1998; Peric, 1993; Poulikakos and Bejan, 1983; Salmun, 1995; Van Doormaal *et al.*, 1981; Yüncü and Yamac, 1991) is representative of this effort. Despite the papers cited here, it could be categorically stated that the essential effects of optimizing the shape of cavities and/or lowering the maximum wall temperature at the directly heated wall to avoid undesirable "hot spots" are still unknown. To the best knowledge of the authors, no information is available in the vast literature on thermo-fluid dynamics that furnishes the optimal shapes of natural convection cavities *a priori* with the help of shape optimization theory.

2. Conservation equations

The physical system shown in Figure 1(a) [1] consists of air confined to a square cavity in which the left vertical wall receives a uniform heat flux and the right vertical wall dissipates heat by convection to an external fluid (normally atmospheric air). The x and y coordinates are chosen in the respective horizontal and vertical directions. The dimension perpendicular to the plane of the diagram in Figure 1(a) is assumed to be long enough, so that the buoyant airflow may be conceived as two-dimensional. The gravitational acceleration acts perpendicular to the insulated horizontal walls. The above physical system seeks to approximate a practical flow situation related to

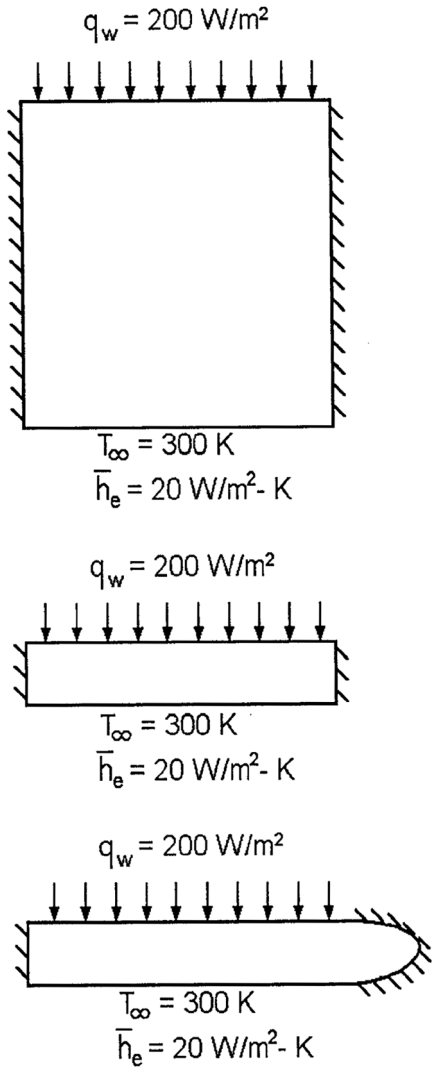

Figure 1.
(a) square cavity;
(b) rectangular cavity; and
(c) capped rectangular cavity

the passive cooling of a tightly-packed array of discrete heat sources that are flush-mounted on the left vertical wall.

In general, the effect of properties changing with temperature is important in natural convection studies because the velocity and temperature fields are interlocked. It is a common practice to assume that the specific heat capacity, the dynamic viscosity and the thermal conductivity of air vary in such a way that the Prandtl number Pr remains constant or at least the average properties can be used in evaluating the Rayleigh and Prandtl numbers. The situation for a cavity filled with an ideal gas ($\mathrm{Pr} = 0.7$) whose dynamic viscosity and thermal conductivity increase with temperature following Sunderland law was examined by Chenoweth and Paolucci (1986). These authors have shown that the Boussinesq approximation gives accurate computations of the overall heat transfer across a differentially heated cavity for temperature ratios $(T_\mathrm{h} - T_\mathrm{c})/T_\mathrm{m} < 0.6$ where $T_\mathrm{m} = (T_\mathrm{h} + T_\mathrm{c})/2$ stands for the mean temperature. Under these premises, the physical properties of the air filling the cavity are taken as temperature-invariant in this work, except for the density which is handled with the Boussinesq approximation. Accordingly, under the assumption of laminar two-dimensional motion, the velocity and temperature fields of incompressible air are described by the following system of conservation equations:

mass:

$$\frac{\partial u}{\partial x} + \frac{\partial v}{\partial y} = 0 \tag{1}$$

x-direction momentum:

$$\frac{\partial (uu)}{\partial x} + \frac{\partial (vu)}{\partial y} = -\frac{1}{\rho}\frac{\partial p}{\partial x} + \nu \frac{\partial^2 u}{\partial x^2} + \nu \frac{\partial^2 u}{\partial y^2} \tag{2}$$

y-direction momentum:

$$\frac{\partial (uv)}{\partial x} + \frac{\partial (vv)}{\partial y} = -\frac{1}{\rho}\frac{\partial p}{\partial y} + \nu \frac{\partial^2 v}{\partial x^2} + \nu \frac{\partial^2 v}{\partial y^2} - g\beta(T_\infty - T) \tag{3}$$

energy:

$$\frac{\partial (uT)}{\partial x} + \frac{\partial (vT)}{\partial y} = \alpha \frac{\partial^2 T}{\partial x^2} + \alpha \frac{\partial^2 T}{\partial y^2} \tag{4}$$

The flow boundary conditions are based on rigid solid walls that are impermeable. The thermal boundary conditions are of mixed type: a uniform heat flux (von Neumann) at the left vertical heated wall and convection (Robin) at the right vertical cooled wall. The two connecting horizontal walls are insulated. For conciseness, the set of flow and thermal boundary conditions are listed in Table I. It should be added that the above physical system is amenable to experimentation because the heat flux boundary condition is easy to establish in the laboratory.

The interaction between natural convection of a fluid confined to a cavity and external convection in an open space through a cavity wall has been examined by Sparrow and Prakash (1981). The development of the boundary layer natural convection in a cavity heated and cooled with a uniform heat flux was documented by

Kimura and Bejan (1984). These two papers are the only ones that are somewhat connected to the cavity problem stated in the preceding subsection. It should be added that the design optimization component was excluded in the two cited works.

3. Numerical computations

An inspection of Table I indicates that the physical domain does not possess thermal symmetry with respect to a vertical axis and inevitably, the physical and computational domains have to coincide. In addition, the non-Dirichlet nature of the four thermal boundary conditions implies that the temperatures along the four straight walls forming the cavity are unknown in advance. Hence, the magnitudes of the wall temperatures must be determined as an integral part of the solution procedure.

The system of four coupled conservation equations (1)-(4), subject to the boundary conditions listed in Table I was solved by the finite-volume procedure (Tannehill *et al.*, 1997). The numerical solution delivers the velocity field in the air subdomain and temperature field in the air/solid subdomain. The commercial CFD code FLUENT (1996) was used for this first phase. Validation of the code results was performed with a well-known benchmark solution for a square cavity having two isothermal vertical walls and two insulated horizontal walls (De Vahl Davis, 1983). Starting with a relatively coarse 30×30 mesh, several mesh sizes were tested for combinations of wall temperature differences and thermo-physical properties of air that are conducive to a Rayleigh number Ra_H that revolves around 10^6. After nondimensionalizing the variables with the scales H, v/H and T_h-T_c, it surfaces up that the numerical solution depends on two parameters: the Rayleigh number Ra and the Prandtl number Pr.

Based on a sequence of numerical experiments for air ($Pr = 0.7$) as the coolant, it was decided that a 60×60 mesh was sufficiently fine so that the velocity and temperature predictions were found to be accurate, dependable and consistent (Table II). The vertical velocity v is the essential variable in the analysis of cavity flows and the estimates for V_{max} are within 5 percent of the results of De Vahl Davis (1983). The convergence criteria of the velocities and temperatures was overseen with the following norm

$$\frac{1}{\phi_{max}} \sqrt{\sum_{i=1}^{N} \left(\phi_i^{n+1} - \phi_i^n\right)^2} \leq \varepsilon \tag{5}$$

where typically $\varepsilon = 10^{-4}$. Further decrease in ε does not cause any significant changes in the results. Therefore, the success of the CFD code in simulating natural convection flows of air in square cavities has been demonstrated. Besides, the overall energy balance, written in terms of the integrated heat transfer rate through each thermally

Location	Velocity	Temperature
Left vertical wall	$u = v = 0$	$-k\,\partial T/\partial x = q_w$
Right vertical wall	$u = v = 0$	$-k\,\partial T/\partial x = h_e(T - T_e)$
Upper horizontal wall	$u = v = 0$	$\partial T/\partial y = 0$
Lower horizontal wall	$u = v = 0$	$\partial T/\partial y = 0$

Table I. Description of the boundary conditions

active wall, must be equal. Agreements to less than 1 percent of the total, average Nusselt number $\overline{Nu}_H$ were found for the aforesaid case. After convergence to the exact velocity and temperature fields was attained, streamlines and isotherms were calculated.

4. Design optimization

4.1 Background

Computational tools for engineering analysis such as CFD codes and structural analysis codes have improved and have become routinely used in designing engineering components. Included in this set of computational tools are powerful computer codes that are commercially available.

Software tools for shape optimization have also matured and proven to be extremely effective for the optimal design of structures (Ding, 1986; Haftka and Granghi, 1986). The maturity of the synergistic combination of tools on engineering analysis with tools on shape optimization still needs improvement for design engineers to be able to fully utilize them in design environments with confidence. As this happens, the design engineer may be able to start with an initial design and allow the "n" number of design variables (including shape change variables) to vary in order to find the best option that complies with the design objectives that exist in the n-dimensional design space. The design space may be constrained by physical limitations (space, weight, etc.) and perhaps by bounds imposed by the design engineer (specifications, requirements, etc.).

To find optimal extrema in the design space, the present study employed a specific optimizer that relies on search algorithms. The specific algorithm utilized here is the gradient-based hybrid sequential quadratic-programming generalized-reduced-gradient (GRG) method (Parkinson and Wilson, 1988). Other search algorithms fall under the category of nongradient based algorithms. However, for the type of problem faced in this work, the GRG algorithm was considered fast, robust, and capable of handling the constraints efficiently.

It is a widely known fact that major components of engineering systems are functions of geometry. The ability to deform the original shapes of such components to arbitrary shapes enhances the design potential of the coupling of engineering analysis software with optimization software. The optimization phase of this study employs an arbitrary shape deformer algorithm that is qualified to change the shape of an initial geometry of a component that needs to be optimized, i.e. the shape of a natural convection cavity in the present study.

Quantity	Present work	De Vahl Davis (1983)
U_{max}	68.81	64.630
Y	0.87	0.850
V_{max}	221.80	217.360
X	0.04	0.038
$Nu_{H,max}$	17.87	17.925
Y	0.04	0.038
$Nu_{H,min}$	1.02	0.989
Y	0.99	1.000
$\overline{Nu}_H$	8.75	8.799

Table II.
Comparison of representative quantities of the velocity and temperature fields of air for $Ra = 10^6$

4.2 Arbitrary shape deformer

The arbitrary shape deformer (ASD) is a powerful sculpting method that deforms a given ambient space. Conceptually, ASD is a generalization of a B-spline volume with the added capability to model a multitude of volumes of general topological structure (Farin, n.d.). ASD is able to produce both local and global deformations using either Bezier functions or nonuniform rational B-spline surfaces (NURBS). The geometry can be defined as computer-aided design data, freeform entities (e.g. Bezier surfaces, NURBS, etc.) or mesh entities (a finite element, a finite volume, etc.). ASD is user-defined to surround the volume containing the model geometry that needs to be optimized. As the ASD's control points are moved, the model geometry experiences gradual deformations. The updated model geometry is then employed as input for the subsequent analysis. The shape deformation algorithm is versatile and delivers enough degrees of freedom to achieve the desired changes in shape. The deformations may range from a fine local to a gross global character using very few shape changes related to the design variables. ASD is numerically stable and delivers the shape optimization for a mesh of high quality without further refinement.

Figure 2 shows a flowchart of the major elements that constitute the design optimization cycle. A major component of this cycle is a suitable commercial computer code for the automatic shape optimization. As mentioned earlier, the first part of this study employed the CFD code FLUENT (1996). For the second part of the study, the shape optimization code OptdesX (1995) is utilized [2]. The latter code possesses several robust and efficient gradient- and non-gradient-based optimization search routines.

Without any exception, it may be reaffirmed that all publications pertinent to natural convection cavities cited in Section 1.1 were limited to a shape of a cavity decided *a priori* without paying attention to its optimal geometric, hydrodynamic and thermal features. On the contrary, the central objective of this investigation is centered in the optimization of the cross-sectional area (volume) of a cavity (without specifying its shape in advance). The desired cavity is subject to a temperature constraint in the

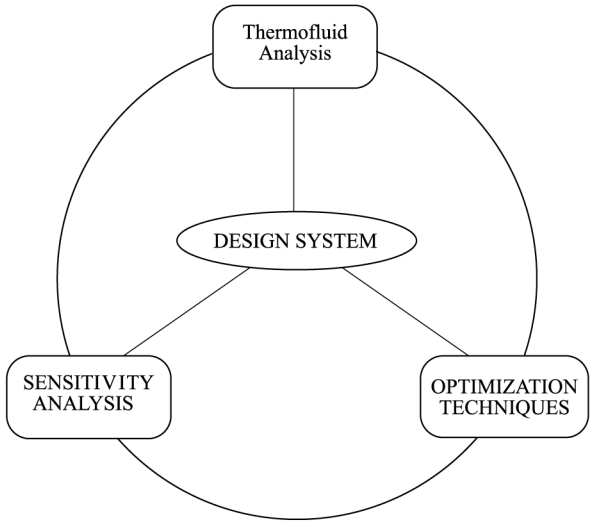

Figure 2.
Design optimization cycle

vertical wall heated with a uniform heat flux. A sequence of two optimization sub-problems is posed as follows.

(1) *First optimization sub-problem*

Find:	shape change control variables
To minimize:	cross-sectional area (volume) of a cavity
Subject to:	(1) An upper limit of the maximum temperature of the directly heated vertical wall
	(2) Shape of four sides to remain straight
	(3) Top and bottom walls remain straight and horizontal

(2) *Second optimization sub-problem*

Find:	shape change control variables
To minimize:	maximum wall temperature of the directly heated vertical wall
Subject to:	(1) Width of cavity to remain constant from the first optimization sub-problem
	(2) Upper insulated wall can be nonstraight
	(3) Bottom insulated wall remains straight and horizontal

5. Optimal design of a cavity

We commence with a conventional initial cavity: a square cavity of cross-sectional area 10×10 cm filled with air ($\mathrm{Pr} = 0.7$) that is shown in Figure 1(a). The set of design parameters is enunciated now: the left vertical wall receives a uniform heat flux of intensity $q_w = 200\ \mathrm{W/m^2}$, the right vertical wall rejects heat to an external fluid and the top and bottom horizontal walls are insulated. The external air temperature is $T_e = 27$°C resulting in an average convective coefficient $\bar{h}_e = 20\ \mathrm{W/m^2\,C}$. These design parameters impart a modified Rayleigh number $\mathrm{Ra_H} = 7 \times 10^7$ to the left vertical wall. The design constraint stipulates that the maximum temperature of the directly heated vertical wall cannot exceed a ceiling value of 137°C.

Accurate velocity and temperature fields have been calculated with a fine 60×60 mesh chosen earlier for the benchmark solution of a square cavity with two isothermal vertical walls and two insulated horizontal walls (De Vahl Davis, 1983).

In the boundary layer regime of a square cavity with uniform heat flux heating, the core is motionless and the temperature linearly stratified (Kimura and Bejan, 1984). From the physics of fluids, it is evident that the velocity of the heated air parallel to the left vertical wall slows down as the fluid approaches the upper left corner. This velocity pattern near the corner is the result of the viscous drag on the fluid caused by the proximity of the insulated horizontal wall. Figures 3(a) and 4(a) show the velocity and temperature fields of the square cavity indicating a maximum velocity of 7.47 cm/s in the vicinity of the upper left corner and a temperature of 127°C at the upper left corner (the "hot" spot). Aside from a palpable large volume of stagnant air that lies in the central part of the square cavity, these two plots are standard and do not need further explanation.

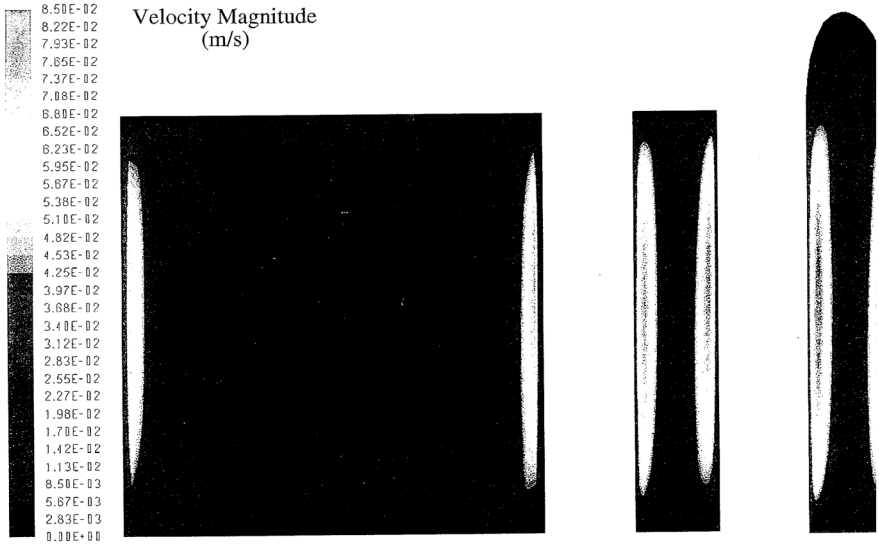

Note: This figure is reproduced from the best original supplied

Figure 3.
Velocity vector plots for: (a) square cavity; (b) rectangular cavity; and (c) capped rectangular cavity

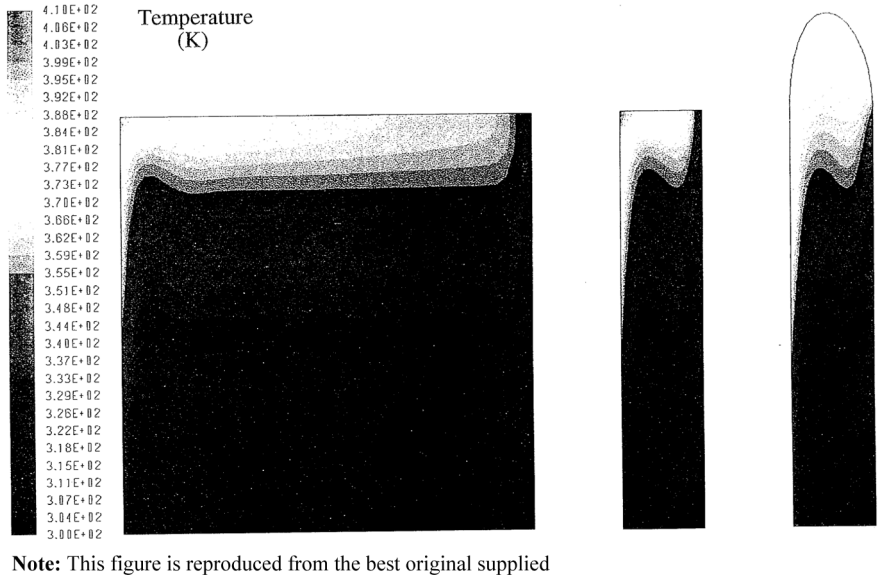

Note: This figure is reproduced from the best original supplied

Figure 4.
Isotherms for: (a) square cavity; (b) rectangular cavity; and (c) capped rectangular cavity

Beginning with the square cavity, the first optimization sub-problem was posed to find a related four-sided cavity of minimum cross-sectional area (volume) with all walls constrained to be straight and the top and bottom insulated walls to remain horizontal. Also, the maximum temperature of the heated vertical wall was constrained to be less

than or equal to a ceiling value of 137°C (a design constraint). In the midst of this, two shape change control variables were defined to allow the right cold vertical wall to move freely in the horizontal plane. One control variable was defined at the upper right corner, while the other control variable was defined at the lower right corner. Subsequently, the shape optimization code OptdesX with the ASD was applied. This step leads to a modification of the two control variables producing at the end the rectangular cavity that is shown in Figure 1(b). As the shape optimizer moved the right cold vertical wall toward the left heated vertical wall, the air mass was compressed appropriately and the square cavity was squeezed. The maximum temperature on the left vertical wall at the upper left corner of the rectangular cavity increased until the wall temperature constraint of 137°C was reached. Figures 3(b) and 4(b) show the velocity and temperature fields of the rectangular cavity (height-to-width ratio $\gg 1$) showing the minimum area (volume) sought. Herein, it is interesting to realize that the optimization algorithm had the necessary degrees of freedom to find a four-sided cavity with arbitrary lengths for the top and bottom insulated walls. In addition, it is important to underline that the stagnation region in the central part of the rectangular cavity has been removed almost completely. Here again, it is worth noting that similar to the square cavity, in a vertical rectangular cavity the air velocity slows down as the fluid approaches the upper left corner. As far as the cavity dimensions are concerned, the final width of the rectangular cavity is merely 2 cm, resulting in a reduced area of 20 cm^2. This area turns out to be a meaningful 80 percent decrease with respect to the area of 100 cm^2 of the original square cavity. Now, the corresponding maximum velocity reached 7.91 cm/s in the vicinity of the upper left corner and the maximum wall temperature at the upper left corner equaled its constrained wall temperature of 137°C.

Given the area (volume) of the rectangular cavity as input, the second optimization sub-problem is posed next. The principal design objective was to find the shape change control variables that alter the shape of the top wall of the rectangular cavity in order to diminish the maximum wall temperature of the left heated wall. Of course, this objective was subjected to maintaining the bottom wall horizontal (related to small velocities) and also to keeping the width of 20 cm unchanged from the first optimization sub-problem. The insulated bottom wall does not need to be adjusted because the physics of fluids suggests that low velocities and low temperatures take place along a path parallel to the bottom wall. The implementation of the optimization code and the ASD involves the definition of two control points for the shape change of the sensitive top insulated wall. Preserving the upper two corner points stationary, two control points are sufficient to define the geometry of the top insulated wall as a cubic spline. The shape of the resulting cavity is shown in Figure 1(c). This new cavity retains the major portion of the rectangular cavity, but is covered with an upper parabolic-skewed insulated cap. The third cavity shape happens to be the optimal cavity shape. At this stage, it should be pointed out that the compromise shape smoothed out both upper left and upper right corners, which were associated with fluid deceleration in the square and rectangular cavities. This round shaped cap negates the abrupt 90° change in fluid direction (from vertical to horizontal) of the upward hot air jet adjacent to the vertical heated wall. Consequently, the upward air jet stays "more parallel" to the vertical heated wall.

This air adherence facilitates the removal of more heat in a marked fashion. The relevance of this localized effect can be confirmed by observing the velocity field plotted in Figure 4(c). In fact, this peculiar behavior has a direct repercussion on the maximum velocity near the old left upper corner, which has now experienced an increment of 8.41 cm/s compared with the maximum velocity for the rectangular cavity (a gain of almost 8 percent).

Figure 3(c) shows the temperature field of the rectangular cavity with an upper insulated parabolic-skewed cap, which turns out to be the optimal cavity. Recall that the maximum wall temperature (the "hot spot") for both square and rectangular cavities took place at the upper left corner. An unexpected beneficial effect of the disfigured optimal cavity is its capability of reducing the maximum wall temperature from 137°C at the upper left corner (in other words at 10 cm from the bottom) of the rectangular cavity to 107°C at a location 8 cm from the bottom.

At this juncture, a one-to-one comparison between the performance of the initial, the intermediate and the final cavities seems to be in order. First, compared to the initial square cavity, the difference in maximum wall temperature represents an huge decrease of 23°C. Second, directing the attention to the cross-sectional area, it is recognizable that the final area for the capped rectangular cavity (optimal cavity) is now 23 cm^2. This size represents a mild increase of 3 cm^2 over the area of the intermediate rectangular cavity, but a dramatic decrease of 77 cm^2 with respect to the original square cavity. Unquestionably, the trade-off between the diminutive gain in area (volume) and the immense reduction of the maximum wall temperature seems to be advantageous from the practical standpoint.

The quantity of foremost importance in the thermal design of cavities with uniform heat flux heating at one vertical wall is the maximum wall temperature that the heated wall can sustain (the "hot spot"). Owing to this, it was deemed appropriate to plot in Figure 5 the variation of the temperatures along the heated vertical wall with height for the three cavities in question. At the lower left corner (the coldest point), the minimum wall temperatures for the three cavities share a common value that is close to 62°C. Irrespective of the shape of the cavity, the wall temperatures rise linearly with height

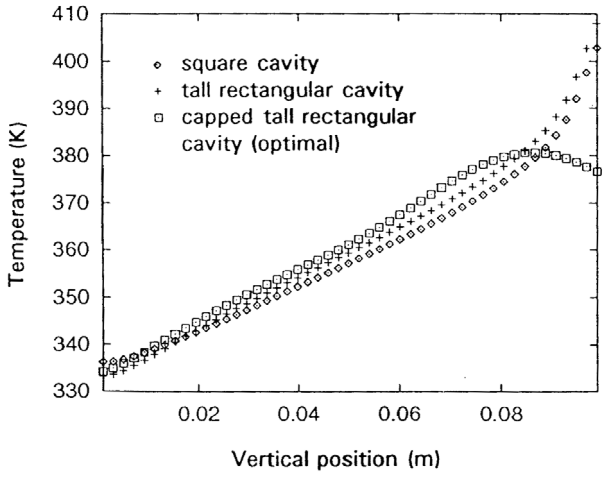

Figure 5.
Temperature variation along the heated vertical wall

up to a location at 8 cm from the bottom. Besides, it is observable that the wall temperature distributions for the three cavities reflect a pattern that is consistent with the relation deduced by Kimura and Bejan (1984):

$$\frac{\nu}{\delta^3} \propto \left(\frac{g\beta}{\nu}\right)\frac{\Delta T}{\delta} \tag{6}$$

where $\Delta T = T_w - T_\infty$ across the boundary layer of thickness δ.

At any height ($0 < y < 10$ cm), the wall temperatures for the capped rectangular cavity (optimal cavity) lie above the wall temperatures for the rectangular cavity. Also, the wall temperatures for the rectangular cavity lie above the wall temperatures for the square cavity. At $y = 8$ cm, the temperatures for both square and rectangular cavities curved up, the former reaching a value of 129°C and the latter reaching even a higher value of 135°C. This linear increase in the temperature was predicted numerically by Kimura and Bejan (1984). The physical explanation for this behavior is that the hot air flow starts to turn away from the vertical direction to the horizontal direction well below reaching the upper left corner; this dissimilarity results in a net convective heat transport reduction in the vicinity of the corner. As expected, the boundary layer breaks down near the upper left corner and near the bottom left corner where the air flows horizontally, and the vertical temperature gradient vanishes.

The first two cavities (with straight walls and four sharp corners) display well-established ascending patterns for the wall temperature. Contrary to this, the wall temperature for the optimal capped rectangular cavity curved down at $y = 8$ cm, passing through a maximum of 107°C at $y = 8$ cm and thereafter decreasing gradually to 105°C at the upper left corner ($y = 10$ cm). The representation in Figure 5 shows quite vividly the impact that the skewed capped shape exerts on the horizontal top wall of the rectangular cavity. Consequently, the addition of a skewed capped wall pays dividends over the horizontal straight wall in providing a favorable trajectory for the movement of the upward hot air jet, pushing down the maximum wall temperature by 20°C as a profitable by-product. Understandably, this thermal/flow/geometric feature is highly desirable from the perspective of the cooling of heat producing electronic components attached to the vertical walls in closed spaces.

The physical explanation for the fluid flow structure of the different shapes of the wall temperature distributions may be done with the help of the scale analysis carried out by Tannehill *et al.* (1997). Here, it was found that inside the thermal boundary layer the air velocity is proportional to the temperature difference. Therefore, it is clear that the presence of the horizontal insulated wall exerts drag on the air upflow jet, causing a deceleration near the upper left corner. Conversely, the upper parabolic-skewed cap creates a favorable path for the air upflow jet, accelerating the flow near the end of the heated vertical wall. This acceleration intensifies the velocity of the air jet removing more heat from the heated wall and bringing the wall temperature down. It may also be speculated that the axial fluid conduction may contribute to the precooling of the wall (Chow *et al.*, 1984).

Certainly, the ability of an air layer to transfer heat inside a cavity may be controlled by altering the shape of the cavity in the regions of high fluid velocities, resulting in an optimal cavity shape. It should be added that if current manufacturing technology precludes the construction of the recommended skewed-cubic cap at an acceptable cost,

a semicircular cap might substitute this characteristic shape. The latter configuration does not deviate markedly from the optimal shape.

To summarize the geometric, velocity and temperature results in a qualitative manner, Table III lists the intrinsic relationship between the three relevant quantities for the three cavities analyzed. The table displays the cross-sectional area, the maximum air velocities in the vicinity of the heated vertical wall and the maximum wall temperatures at the heated vertical wall.

Finally, it should be added that the optimal design of cavities heated and cooled at the sidewalls responds to a specific set of design parameters, namely: the working fluid is air, a uniform wall heat flux, $q_w = 200\,W/m^2$, convection to an external fluid with temperature $T_e = 25°C$ and an average convective coefficient $\bar{h}_e = 20\,W/m^2\,C$. The maximum wall temperature at the heated wall was constrained at a ceiling value of 137°C. Perhaps, the design engineer may expect minor changes in the optimal design of the cavity for a different set of design parameters and design constraints. Certainly, the groundwork is set for future applications of the CFD-shape optimization united methodology to solve a wide variety of problems in fluid-filled natural convection inside cavities.

6. Conclusions

Relying on the numerical results that articulate concepts of fluid dynamics, heat transfer and shape optimization, the conclusions that can be drawn from this work are enumerated as follows.

(1) The output of a CFD in terms of velocity and temperature fields in a natural convection square cavity code provides the necessary input for a shape optimization code to perform automatic optimization of the shape of the cavity in harmony with the pre-established design parameters and design constraints.

(2) The shape optimization code proved to be an efficient tool in molding the cross-sectional area of a natural convection cavity heated with a uniform heat flux from the side. As a result, the upward airflow near the directly heated vertical wall was forced to take a more efficient path, diminishing the maximum wall temperatures along the heated vertical wall (the "hot spot").

(3) It has been demonstrated that the miniaturization of natural convection cavities constrained by maximum allowable wall temperatures at the "hot spot" is feasible and also can be done in an optimal way.

Shape of cavity	Cross-sectional area (cm^2)	Maximum air velocity (cm/s)	Maximum wall temperature (°C)
Square	100	7.49	127
Rectangular	20 (−80)	7.91 (+0.42)	137 (+10)
Capped rectangular (optimal shape)	23 (−77)	8.41 (+0.92)	107 (−20)

Note: [a]The numbers in parentheses represent deviations experienced by a quantity in a nonsquare cavity relative to the original square cavity during the course of the shape optimization

Table III. Comparison between the initial, intermediate and final configurations of the cavities[a]

Notes

1. Color plots may be found in the Web site: www.emba.uvm.edu/~acampo.
2. The mesh was the definite mesh employed for the calculation of the velocity and temperature fields.

References

Akinsete, V.A. and Coleman, T.A. (1982), "Heat transfer by steady laminar free convection in triangular enclosures", *Int. J. Heat Mass Transfer*, Vol. 25, pp. 991-8.

Asako, Y. and Nakamura, H. (1982), "Heat transfer in a parallelogram shape enclosure", *Bull. JSME*, Vol. 25, pp. 1419-27.

Batchelor, G.K. (1954), "Heat transfer by free convection across a closed cavity between vertical boundaries at different temperatures", *Quart. Appl. Math.*, Vol. 12, pp. 209-33.

Chang, L.C., Lloyd, J.R. and Yang, K.T. (1982), "A finite difference study of natural convection in complex enclosures", *Heat Transfer 1982: Proc. 7th Int. Heat Transfer Conf.*, Munich, Germany, Vol. 2, pp. 183-8.

Chenoweth, D.R. and Paolucci, S. (1986), "Natural convection in an enclosed vertical air layer", *J. Fluid Mech.*, Vol. 169, pp. 173-210.

Chow, L-C., Campo, A. and Husain, S. (1984), "Effects of free convection and axial fluid conduction heat transfer inside a vertical channel at low peclet numbers", *ASME J. Heat Transfer*, Vol. 106, pp. 297-303.

Chung, K.C. and Trefethen, L.M. (1982), "Natural convection in a vertical stack of inclined parallelogrammic cavities", *Int. J. Heat Mass Transfer*, Vol. 25, pp. 277-84.

De Vahl Davis, G. (1983), "Natural convection of air in a square cavity: a benchmark numerical solution", *Int. J. Numer. Meth. Fluids*, Vol. 11, pp. 249-64.

Ding, Y. (1986), "Shape optimization of structures – a literature review", *Computers and Structures*, Vol. 24, pp. 985-1004.

Eckert, E.R.G. and Carlson, W.O. (1961), "Natural convection in an air layer enclosed between two vertical plates with different temperatures", *Int. J. Heat Mass Transfer*, Vol. 2, pp. 106-13.

Elder, J.W. (1965), "Laminar free convection in a vertical slot", *J. Fluid Mech.*, Vol. 23, pp. 77-98.

Facas, G.N. (1993), "Laminar free convection in a non-rectangular inclined cavity", *AIAA J. Thermophysics Heat Transfer*, Vol. 7, pp. 447-53.

Farin, G. (n.d.), *Curves and Surfaces for Computer-Aided Geometric Design, A Practical Guide*, 4th ed., Academic, San Diego, CA.

Fluent Reference Manual (1996), FLUENT Inc., Lebanon, NH.

Gebhart, B., Jaluria, Y., Mahajan, R.L. and Sammakia, B. (1988), *Buoyancy-Induced Flows and Transport*, Hemisphere, New York, NY.

Haftka, R.T. and Granghi, R.V. (1986), "Structural shape optimization – a survey", *Comput. Meth. Appl. Mech. Engng.*, Vol. 57, pp. 91-106.

Holtzman, G.A., Hill, R.W. and Ball, K.S. (2000), "Laminar natural convection in isosceles triangular enclosures heated from below and symmetrically cooled from above", *ASME J. Heat Transfer*, Vol. 122, pp. 485-91.

Hyun, J.M. and Choi, B.S. (1990), "Transient natural convection in a parallelogram-shaped enclosure", *Int. J. Heat Fluid Flow*, Vol. 11, pp. 129-34.

Iyican, L., Bayazitoglu, Y. and Witte, L.C. (1980a), "An analytical study of natural convective heat transfer within a trapezoidal enclosure", *ASME J. Heat Transfer*, Vol. 102, pp. 640-7.

Iyican, L., Bayazitoglu, Y. and Witte, L.C. (1980b), "An experimental study of natural convection in trapezoidal enclosure", *ASME J. Heat Transfer*, Vol. 102, pp. 648-53.

Karyakin, Y.E., Sokovishin, A. and Martynenko, O.G. (1988), "Transient natural convection in triangular enclosures", *Int. J. Heat Mass Transfer*, Vol. 31, pp. 1759-66.

Kim, G.B. and Hyun, J.M. (1999), "Buoyant convection in a non-rectangular cavity with non-vertical insulating sidewalls", *Int. J. Heat Mass Transfer*, Vol. 42, pp. 2111-17.

Kimura, S. and Bejan, A. (1984), "The boundary layer natural convection regime in a rectangular cavity with uniform heat flux from the side", *ASME J. Heat Transfer*, Vol. 106, pp. 98-103.

Lam, S.W., Gani, R. and Symons, J.G. (1989), "Experimental and numerical studies of natural convection in trapezoidal cavities", *ASME J. Heat Transfer*, Vol. 111, pp. 372-7.

Lee, T.S. (1984), "Computational and experimental studies of convective fluid motion and heat transfer in inclined non-rectangular enclosures", *Int. J. Heat Fluid Flow*, Vol. 5, pp. 29-36.

Lee, T.S. (1991), "Numerical experiments with fluid convection in tilted non-rectangular enclosures", *Numer. Heat Transfer, Part B*, Vol. 9, pp. 487-99.

Maekawa, T. and Tanasawa, I. (1982), "Natural convection heat transfer in a parallelogrammic enclosure", *Heat Transfer 1982: Proc. 7th Int. Heat Transfer Conference*, Munich, Germany, Vol. 2, pp. 227-32.

Naylor, D. and Oosthuizen, P.H. (1994), "A numerical study of free convective heat transfer in a parallelogram-shaped enclosure", *Int. J. Numer. Meth. Heat Fluid Flow*, Vol. 4, pp. 553-9.

Nithiarasu, P., Sundarajanan, T. and Seetharamu, K.N. (1998), "Finite element analysis of transient natural convection in an odd-shaped enclosure", *Int. J. Num. Meth. Heat Fluid Flow*, Vol. 8, pp. 199-216.

OptdesX Reference Manual (1995), *A Software System for Optimal Engineering Design*, Design Synthesis, Inc., Provo, UT.

Parkinson, A. and Wilson, M. (1988), "Development of a hybrid SQP-GRG algorithm for constrained non-linear programming", *ASME J. Mechanisms Transmissions Automation in Design*, Vol. 110, pp. 308-15.

Peric, M. (1993), "Natural convection in trapezoidal cavities", *Numer. Heat Transfer, Part B*, Vol. 24, pp. 213-19.

Peterson, G.P. and Ortega, A. (1990), "Thermal control of electronic equipment and devices", *Advances in Heat Transfer*, Vol. 20, Academic, New York, NY, pp. 181-314.

Poulikakos, D. and Bejan, A. (1983), "The fluid mechanics of an attic space", *J. Fluid Mech.*, Vol. 131, pp. 251-69.

Raithby, G.D. and Hollands, K.G.T. (1998), "Natural convection", in Rohsenow, W.M., *et al.* (Eds), *Handbook of Heat Transfer*, 3rd ed., Chapter 4, McGraw-Hill, New York, NY.

Salmun, H. (1995), "Convection patterns in a triangular domain", *Int. J. Heat Mass Transfer*, Vol. 38, pp. 351-62.

Sparrow, E.M. and Prakash, C. (1981), "Interaction between internal natural convection in an enclosure and an external natural convection boundary layer flow", *Int. J. Heat Mass Transfer*, Vol. 24, pp. 895-907.

Tannehill, J.C., Anderson, D.A. and Pletcher, R.H. (1997), *Computational Fluid Mechanics and Heat Transfer*, Taylor and Francis, Washington, DC.

Van Doormaal, J.P., Raithby, G.D. and Strong, A.B. (1981), "Prediction of natural convection in non-rectangular enclosures using orthogonal curvilinear coordinates", *Numer. Heat Transfer*, Vol. 4, pp. 21-38.

Yüncü, H. and Yamac, S. (1991), "Laminar natural convective heat transfer in an air-filled parallelogramic cavity", *Int. Comm. Heat Mass Transfer*, Vol. 18, pp. 559-68.